Langmuir – Blodgett Assembly of One-Dimensional Nanostructures

Peidong Yang* and Franklin Kim[a]

The Langmuir – Blodgett technique has been used to assemble one-dimensional nanoscale building blocks. Various superstructures can be obtained as a result of different interactions between the individual nanostructures and different surface pressure applied. The general assembly behavior is exemplified here with $BaCrO_4$, $BaWO_4$, Au nanorods, and $Mo_3Se_3^-$ nanowires.

KEYWORDS:

Langmuir – Blodgett films · liquid crystals · nanorods · nanostructures · nanowires

From a chemist's point of view, nanoscale science is all about assembling matter at multiple length scales from atomic and molecular species to individual nanoscale building blocks, such as nanocrystals, nanorods, and nanowires, then from these individual nanoscale building blocks to higher-level functional assemblies and systems. This hierarchical process covers a length scale of several orders, from Ångströms to micrometers or larger. The past decades have witnessed great progress in the direction of synthesizing nanocrystals of various composition, sizes, and shapes.[1–7] A grand challenge, however, resides in the hierarchical integration of the nanoscale building blocks into functional assemblies and ultimately into a system. Unlike the traditional lithographical process, where precise placement of certain elements or devices is embedded in the design process, the precise placement of nanoscale building blocks at the right place with right configuration and with exceedingly high densities represents a daunting task for researchers in this field.

Nanotubes, nanowires, and nanorods represent a very unique class of one-dimensional (1D) nanoscale building blocks. Once such one-dimensional nanoscale building blocks can be ordered and rationally assembled into appropriate two- or three-dimensional architectures, they will offer fundamental scientific opportunities for investigating the influence of size and dimensionality with respect to their collective optical, magnetic, and electronic properties. Current efforts have been focused on the development of new synthetic methodologies (for example reverse micelle templating, seed-mediated growth, crystal growth regulated by surfactant and co-surfactant, and magic-sized nucleation and growth)[1–9] for making nanorods with uniform sizes and aspect ratio. Few studies addressed the organization of these anisotropic building blocks except the spontaneous three-dimensional superlattice formation of $BaCrO_4$, FeOOH, CdSe, Co, Ag, and Au nanorods.[1–9]

The Langmuir – Blodgett (LB) technique is a quite powerful assembly approach with several unique characteristics. First, a large area of ordered nanocrystal monolayer can be formed, which can be easily transferred to other substrates, and it is also fairly easy to carry out multiple or alternating layer deposition. In addition, the interparticle distance and the final superstructures can be finely tuned through control of the compression process, which could result in a wide range of properties such as the insulator-to-metal transition observed for a monolayer of silver nanocrystals.[8, 9]

Previously, Langmuir – Blodgett films of various nanoparticles such as Ag, Au, and CdS have been prepared.[8, 9] Typically, the surface of the nanocrystals are functionalized by organic molecules (usually long alkyl chains) in order to prevent particle aggregation and also to ensure the nanoparticles float on the subphase surface (usually water). The nanoparticles are dispersed in organic solvents such as toluene, and this solution is spread dropwise onto the subphase surface. The nanoparticles form a monolayer on the water – air interface, which is slowly compressed. This monolayer can be transferred during the compression process using either horizontal or vertical liftoff to substrates such as transmission electron microscopy (TEM) grids or silicon wafers in order to be inspected with electron and optical microscopy. James Heath et al. have done extensive studies on Langmuir – Blodgett films of silver and gold nanoparticles.[8, 9] For spherical nanoparticles, the particles form a gaslike phase at low densities, where the monolayer is highly compressible without significant increase in the surface pressure. Depending on the particle size, the length of the capping ligand, and the surface pressure, various microscopic structure of islands, wires, and rings composed of the nanoparticles can be formed. As the monolayer is compressed, they start to form a condensed phase, usually a hexagonally close-packed structure due to the isotropic interparticle interactions. At this stage, the interparticle separation distance decreases with increased compression. This raises the possibility of obtaining a range of controllable properties that can be finely tuned without extreme conditions such as high temperature and pressure. For example, the Heath group observed an insulator-to-metal transition when

[a] *Prof. P. Yang, F. Kim*
Department of Chemistry
University of California
Berkeley, CA 94720 (USA)
Fax: (+1) 510-642-7301
E-mail: p_yang@uclink.berkeley.edu

the monolayer of silver particles is compressed sufficiently so that the energy gain from the electron delocalization is significant enough to overcome the single particle charging energy.[8]

Recently, we have successfully applied the Langmuir–Blodgett technique to the assembly of one-dimensional nanostructures such as nanorods and nanowires.[10, 11] These 1D nanostructures are rendered hydrophobic by surfactant surface functionalization before the LB experiments. Figure 1 schematically shows the experimental apparatus. The surface pressure π follows a $\pi - A$ (area) curve, Figure 2, that is commonly observed during the LB compression of amphiphilic surfactants or surfactant capped nanoclusters on the water surface.[12] Superstructure formation from these anisotropic nanoparticles, however, displays much more complex behavior than the spherical particles, as have been demonstrated in our experiments with $BaCrO_4$, $BaWO_4$, Au nanorods, and $Mo_3Se_3^-$ nanowires. Superstructure formation is highly dependent on the aspect ratio of the nanorods and the collective interactions among these individual units.

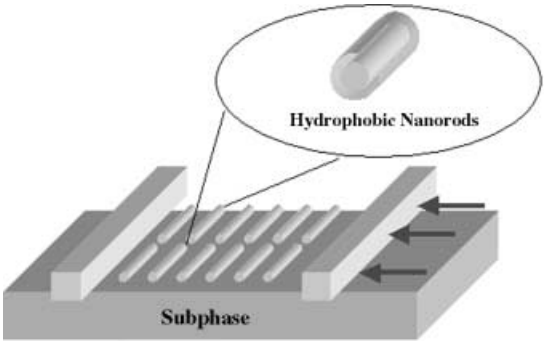

Figure 1. *Schematic illustration of the Langmuir–Blodgett apparatus for nanorod assembly. Nanorods are generally rendered hydrophobic through surface functionalization.*

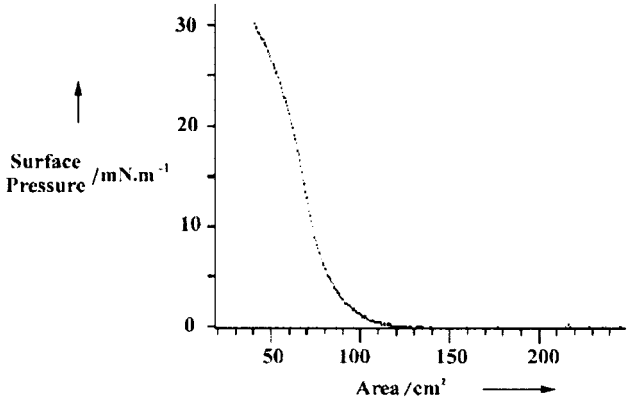

Figure 2. *Typical Langmuir isotherm (surface pressure versus area) during the nanorod compression.*

For nanorods with small aspect ratio ($\sim 3-5{:}1$) such as the $BaCrO_4$ nanorods (diameters ~ 5 nm), they form raftlike aggregates of generally three to five rods by aligning side-by-side due to the directional capillary force and the van der Waals attraction at low densities (equivalently low surface pressure). These aggregates are dispersed on the subphase surface in a mostly isotropic state (Figure 3A). As the monolayer is compressed, the nanorods start to align into a certain direction and form a nematic phase. With further compression, nanorod assemblies with smectic arrangement are obtained (Figure 3B), which is characterized by layer-by-layer stacking of ribbonlike nanorod superstructures. During this compression, the areal density of the nanorods also increases significantly, from ~ 500 to $\sim 5000\ \mu m^{-2}$. Above a certain pressure, the monolayer breaks into multilayers, where it resumes a disordered three-dimensional nematic configuration (Figure 3C). The overall nematic arrangement in the multilayer nanorod superstructures is frequently disrupted by singularities such as disclinations. Figure 4 shows two typical examples of the disclinations with strength[*] s of $+1$, where we see the director of individual nanorods changes continuously about the disclinations. In liquid crystal literature, these *Schlieren* textural defects are commonly observed under polarized optical microscopy as a microscopic manifestation of molecular director rotation.

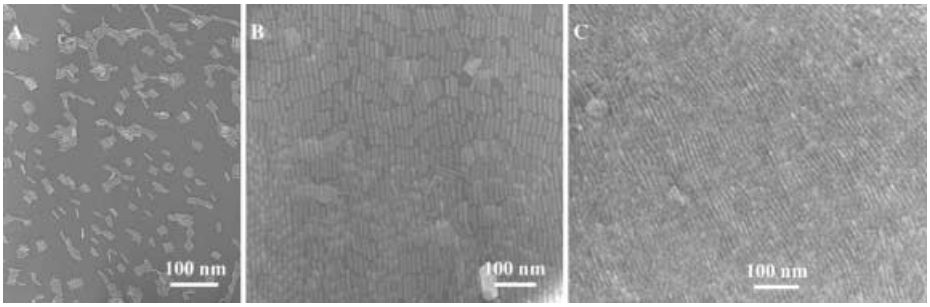

Figure 3. *TEM images of $BaCrO_4$ nanorod arrangement at different stages of compression.*

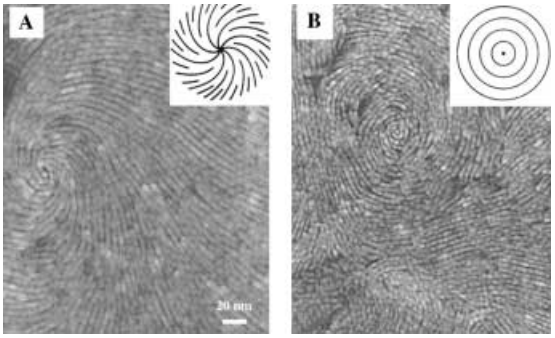

Figure 4. *TEM images for textural defects within the multilayer nanorods. Both defects have a strength s of $+1$. Inset: The nanorod director orientation in the vicinity of disclinations. Reprinted with permission from ref. [10], copyright American Chemical Society, 2001.*

[*] *(Disclination) strength, in this case, is defined as the number of rotations by 2π of the director around the center of the defect. Strength is a measure of topological stability and light-scattering facility.*

This LB technique was also applied to the thiol-capped gold nanorods (diameters $\sim$8 nm) of similar aspect ratio. However, these metal nanorods have a great tendency to form nanorod ribbons spontaneously. In these nanoribbon superstructures, many gold nanorods align side-by-side. Compression of these nanorod monolayers does not exhibit the same phase evolution as seen in the $BaCrO_4$ system. In most cases, isotropic arrangements of the gold nanorod ribbon structures are "quenched" during the compression (Figure 5). This difference can be attributed to the much greater attractive van der Waals and directional capillary interaction among gold nanorods as compared with the $BaCrO_4$ nanorods as well as the polydispersity of the available gold nanorods.

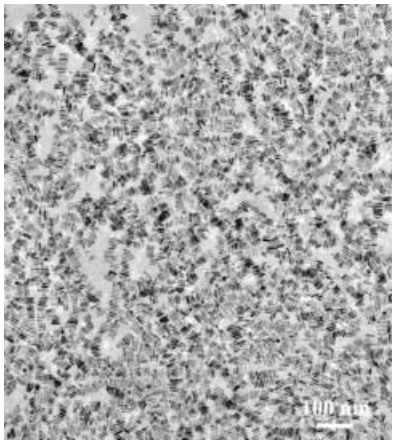

Figure 5. *TEM image of the arrangement of Au nanorods after compression.*

On the other hand, the organization of the $BaWO_4$ nanorods (diameter $\sim$10 nm) with large aspect ratio ($\sim$150:1) again differs significantly from the assembly of the short $BaCrO_4$, Au, and CdSe nanorods where ribbonlike and vertical rectangular or hexagonal superstructures are often favored. With low surface pressure, these nanorods are fairly dispersed; the directors of the nanorods are isotropically distributed, and no superstructures can be observed. After compression, these nanorods readily align in roughly the same direction and form a nematic layer (Figure 6). With strong compression, these nanorods form bundles that have almost perfect side-by-side alignment between the included nanorods.[11] The preference of nematic phase formation upon compression is a distinct characteristic of the assembly behavior for nanorods with a large aspect ratio. This has also been clearly observed in another molecular wire system $Mo_3Se_3^-$ (diameter 0.8 nm, aspect ratio effectively infinite) in our lab.

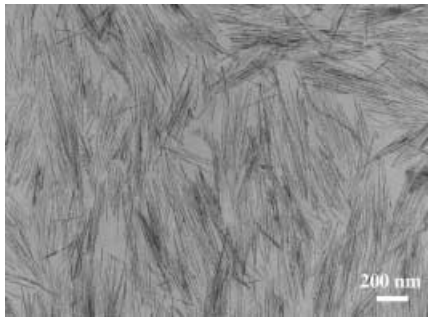

Figure 6. *TEM images of the $BaWO_4$ nanorods assemblies at an air – water interface after compression at relative high surface pressure. Reprinted with permission from ref. [11], copyright Royal Society of Chemistry, 2001.*

It should be mentioned that the organization of the nanorods here is quite different from those of the spherical nanoparticles where a hexagonally close-packed lattice is preferred due to isotropic interparticle interactions. In the current experiments, a nanorod includes an inorganic core surrounded by the surfactants. Consider a fluid of such long, thin rods without any forces between them other than the one preventing their interpenetration (hard rod approximation); at sufficiently low densities, the rods can assume all possible orientations and the fluid will be isotropic (Figure 7). As the density increases, it becomes increasingly difficult for the rods to point in random directions and intuitively one may expect the fluid to undergo a transition to a more ordered anisotropic phase having uniaxial symmetry (Figure 7). This ordering occurs in order to maximize the entropy of the self-assembled structure by minimizing the excluded volume per particle in the array as first proved by Lars Onsager.[13] Indeed, Daan Frenkel et al. have carried out Monte Carlo simulations[14] on the phase behavior of two-dimensional hard rod fluids, which show strong correlations with our experimental data despite the fact that our nanorods are not ideal hard rods. This entropy argument also explains the great tendency for large aspect ratio 1D nanostructures, such as the $BaWO_4$ rods and $Mo_3Se_3^-$ molecular wires, to form nematic structures.

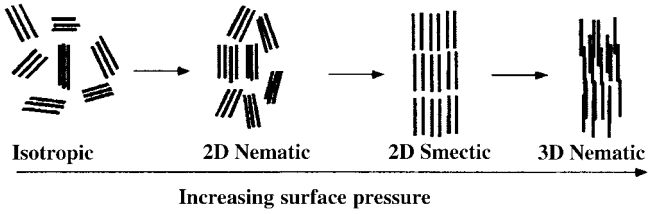

Figure 7. *Schematic illustration of the pressure-induced phase transition when the nanorods with shorter aspect ratios are compressed at the water – air interface. Reprinted with permission from ref. [10], copyright American Chemical Society, 2001.*

In addition, the assembly behavior of realistic nanorods would deviate from those of ideal hard rods due to the existence of significant van der Waals interaction and directional capillary interaction. Strictly, none of our experimental 1D nanostructures can be considered as ideal hard rods. For example, in explaining the tendency of nanorods to align parallel to each other, another reason would be the higher lateral capillary forces along the length of a nanorod as compared to its width. This anisotropy of interaction between nanorods could be one important driving force for the side-by-side, rather than end-to-end, alignment of nanorods. It is also true that between any two bodies of matter

there is an attractive van der Waals force caused by the interaction between the fluctuating electromagnetic fields associated with their polarizabilities. The attraction between two atoms separated by distance r goes as r^{-6} (the Lennard-Jones potential) and the interaction between two spherical particles of radius R, obtained by summing over all pairs of atoms, is given by Equation (1), where r is now the center-to-center separation.

$$V_A(r) = -\frac{A}{6}\left[\frac{2R^2}{r^2 - 4R^2} + \frac{2R^2}{r^2} + \ln\left(1 - \frac{4R^2}{r^2}\right)\right] \quad (1)$$

The strong directional capillary and van der Waals interaction between the gold nanorods explains well why their two-dimensional assembly process deviates significantly from the ideal hard rod system.

While the existence of strong attractive interactions among the nanorods would complicate their assembly process, it should be recognized that these interactions can also be systematically tuned in order to form desired nanorod superstructures. For example, the Hamaker constant A in the van der Waals attraction term is determined by the material properties of the particles and suspension medium, in particular their frequency-dependent polarizabilities. Of relevance here is if the particles and liquid have equal polarizabilities, then $A = 0$. Thus if the refractive indices of the particles and liquid are matched, van der Waals attractions are expected to be negligible. Consequently, the interaction between the nanorods can be modified as desired.

The two-dimensional assembly behavior of the one-dimensional nanostructures is quite complex and is highly dependent on their sizes and aspect ratios. The surface functionality of the these one-dimensional nanostructures plays significant roles in regulating the attractive and repulsive interactions among these individual units, consequently determining their final two- or three-dimensional superstructures. Aligning these one-dimensional nanoscale building blocks into nematic or smectic phases has its significance in both fundamental studies of the structure – properties correlation of nanostructures and the technologically important areas such as formation of high density logic and memory devices.

P.Y. acknowledges the NSF, DOE, and Hellman Family Foundation for support of this work.

[1] a) X. Peng, L. Manna, W. Yang, J. Wickham, E. Scher, A. Kadavanich, A. P. Alivisatos, *Nature* **2000**, *404*, 59; b) V. F. Puntes, K. M. Krishnan, A. P. Alivisatos, *Science* **2001**, *291*, 2115.
[2] S. Chang, C. Shih, C. Chen, W. Lai, C. R. C. Wang, *Langmuir* **1999**, *15*, 701.
[3] M. Li, H. Schnablegger, S. Mann, *Nature* **1999**, *402*, 393.
[4] N. R. Jana, L. Gearheart, C. J. Murphy, *Chem. Commun*. **2001**, 617.
[5] S. J. Park, S. Kim, S. Lee, Z. G. Khim, K. Char, T. Hyeon, *J. Am. Chem. Soc*. **2000**, *122*, 8581.
[6] B. Nikoobakht, Z. L. Wang, M. A. El-Sayed, *J. Phys. Chem. B* **2000**, *104*, 8635.
[7] H. Maeda, Y. Maeda, *Langmuir* **1996**, *12*, 1446.
[8] C. P. Collier, R. J. Saykally, J. J. Shiang, S. E. Henrichs, J. R. Heath, *Science* **1997**, *277*, 1978.
[9] S. W. Chung, G. Markovich, J. R. Heath, *J. Phys. Chem. B* **1998**, *102*, 6685.
[10] F. Kim, S. Kwan, J. Akana, P. Yang, *J. Am. Chem. Soc.* **2000**, *122*, 4360 – 4361.
[11] S. Kwan, F. Kim, J. Arkana, P. Yang, *Chem. Commun.* **2001**, *5*, 447.
[12] C. Messerschmidt, A. Schulz, J. Zimmermann, J. Fuhrhop, *Langmuir* **2000**, *16*, 5790.
[13] a) L. Onsager, *Ann. N.Y. Acad. Sci.* **1949**, *51*, 627; b) G. J. Vroege, H. N. W. Lekkerkerker, *Rep. Prog. Phys*. **1992**, *55*, 1241.
[14] a) J. A. C. Veerman, D. Frenkel, *Phys. Rev. A: At., Mol., Opt. Phys.* **1991**, *43*, 4334; b) M. A. Bates, D. Frenkel, *J. Chem. Phys*. **2000**, *112*, 10034.

Received: January 7, 2002 [C355]